Effect of a polarized hydrogen target on the polarization of a stored proton beam

H. O. Meyer
Department of Physics, Indiana University, Bloomington, Indiana 47405
(Received 22 February 1994)

We investigate the change of polarization of a stored proton beam induced by the presence of an internal, polarized, atomic hydrogen target. Three distinct mechanisms are identified that significantly contribute to the beam polarization. The calculated polarization rate agrees with the result of a recent experiment.

PACS number(s): 29.20.Dh, 29.25.Pj, 29.27.Hj, 25.40.Cm

I. INTRODUCTION

A. Polarized beams and targets in storage rings

In recent years, storage rings [1] have clearly demonstrated their potential as a tool in nuclear physics research, especially in few-body reactions. If a means of phase space cooling is employed, it is feasible to carry out experiments by placing an internal target in the path of the stored beam. The optimum target thickness d is given by the cooling force. For a medium-energy beam and a hydrogen target, for example, d is a few times 10^{14} atoms per cm^2.

Polarized hydrogen gas targets of the appropriate thickness can be produced by means of an atomic beam source. Since the production rate of polarized H atoms even by the best atomic source is rather small (less than 10^{17} atoms/s), a so-called buffer cell is used to increase the dwell time of target atoms near the beam. Such a cell is simply a narrow tube through which the stored beam passes [2]. The polarized atoms enter through another tube, pointing sideways, which is connected to the center of the first and which is aligned to the beam axis of the polarized atomic beam source.

In order to exploit the possibilities of internal, polarized targets, the beam also has to be polarized. Usually, the polarized beam is supplied by a polarized ion source, then accelerated and injected into the ring using techniques of phase space stacking with concurrent cooling. However, other methods to provide polarized beam are conceivable. In medium-energy storage rings [1] beam particles can be stored for hours, orbiting with frequencies of the order of 1 MHz. Thus, it may be possible that additive spin-dependent interactions, even if they are small, could lead to beam polarization. This would be especially interesting for particles for which no polarized sources exist (such as antiprotons). For example, in the proposed, so-called "spin splitter method" [3], inhomogeneous magnetic fields would be used to gradually split the stored beam into components of given magnetic substates. This method is still waiting for an experimental proof. Another method to polarize a storage beam, also known as the "filter method", utilizes the spin-dependent interaction of the stored ions with a polarized, internal target. Such an effect has recently beam demonstrated with the Test Storage Ring (TSR) at the Max Planck Institut for Nuclear Physics in Heidelberg. Since the TSR experiment provided the motivation for the present paper, it is briefly summarized in Sec. I B. The remainder of the paper is a study of the effect of a polarized, internal, atomic hydrogen target on a stored, cooled proton beam.

B. TSR spin-filter experiment

For the TSR experiment, a 23-MeV stored proton beam interacted with an internal target of about 6×10^{13} polarized hydrogen atoms per cm^2. The target was polarized vertically (perpendicular to the ring plane). It was prepared in a pure, atomic spin state with protons and electrons polarized in the same direction. The beam lifetime without the target was about 300 min; with the target it decreased to about 30 min. The beam was left to orbit with the target in place for times between 30 and 90 min; then the polarization was measured. It was found that the stored beam acquired a polarization P_B of the same sign as the polarized target, at a rate of $dP_B/dt=0.0124\pm0.0006$ per h [4].

In Ref. [4], it was argued that the beam polarizes because its two spin states are depopulated unevenly, because, at 23 MeV, the total cross section for scattering of protons with spins aligned in the same direction is much smaller than if their spins are opposite (hence the name filter method). Based on this idea, using the measured ring acceptance angle $\theta_{\rm acc}=4.4\pm0.5$ mrad [5] and the known, spin-dependent total $p+p$ cross section, a polarizing rate of $(dP_B/dt)_{\rm theor}=0.024$ per h was calculated [4]. This expectation is about twice the measured value. It was argued that a finite polarization lifetime would explain such a discrepancy but no plausible depolarization mechanism could be identified. From the result of the present paper it will become clear that the interpretation of Ref. [4] is too simple and that the observed polarization rate is, in fact, what one would expect.

II. THE POLARIZING CROSS SECTION $\hat{\sigma}$

A. Definition of $\hat{\sigma}$

Consider a beam of spin-$\frac{1}{2}$ particles orbiting with frequency f_R in a ring. We denote the time-dependent

beam polarization by $P_B(t)$. The numbers of stored protons in the two spin states are $N_\uparrow$ and $N_\downarrow$, where the arrow denotes the sign of the magnetic substate with respect to the quantization axis. The beam polarization can then be expressed as

$$P_B=\frac{N_\uparrow-N_\downarrow}{N_\uparrow+N_\downarrow} . \tag{1}$$

By taking the derivative with respect to time and rearranging terms, one finds

$$\frac{dP_B}{dt}=(1-P_B^2)\frac{1}{2}\left[\frac{1}{N_\uparrow}\frac{dN_\uparrow}{dt}-\frac{1}{N_\downarrow}\frac{dN_\downarrow}{dt}\right] . \tag{2}$$

The derivatives dN/dt may be nonzero either because stored protons are lost or because their spin is flipped.

We now assume the presence of a polarized, internal, atomic hydrogen target of polarization P_T (constant) and of thickness d (nuclei per cm^2). The effect of this target on the beam polarization must be proportional to its polarization P_T, its thickness d, and the orbit frequency f_R. The constant of proportionality, which has the dimension of an area, we will call "the polarizing cross section $\hat{\sigma}$". One thus can write

$$\frac{dP_B}{dt}=(1-P_B^2)f_R dP_T\hat{\sigma} . \tag{3}$$

The sign of $\hat{\sigma}$ determines whether the change of beam polarization is in the direction of the target polarization or opposite. By solving the differential equation Eq. (3), one obtains the time dependence of the beam polarization:

$$P_B(t)=\tanh(tf_R dP_T\hat{\sigma}) . \tag{4}$$

In the following we will discuss the polarizing cross section $\hat{\sigma}$ as it arises from the interaction of protons with polarized hydrogen atoms. As we will see, there are three distinct mechanisms that contribute significantly to $\hat{\sigma}$.

By convention, we will use the basis vectors $\hat{l}$ (longitudinal), $\hat{n}$ (normal to the scattering plane), and $\hat{m}$ (sideways, completing a right-handed coordinate system). Angles and other kinematical variables are in the laboratory system if they are marked with an asterisk; otherwise the center-of-mass system is used. Throughout, we will use $c=\hbar=1$. We will consider two special choices for the polarization direction of the target, namely along the beam direction (longitudinal, symbol $||$) or perpendicular to the ring plane (transverse, symbol $\perp$). The definitions of polarization observables are consistent with the conventions used in Ref. [6].

B. Contribution of beam proton removal: $\hat{\sigma}_R$

We restrict this discussion to beam energies below the pion-production threshold, where the $p+p$ interaction is purely elastic. A beam proton that scatters from a target proton is removed from the stored beam if the scattering angle is so large that the beam particle is no longer contained within the machine acceptance. We assume that for a given target location there is a well-defined, limiting scattering angle $\Theta_{\rm acc}$, such that when it is exceeded, loss occurs. This assumption is true for a beam of small emittance, a condition which is likely to be met when (relatively thin) polarized targets are used. Because of the spin dependence of $p+p$ scattering, the removal probabilities of beam protons in the $\uparrow$ and $\downarrow$ spin states differ. We denote the cross sections for particle removal by $\sigma(\uparrow\uparrow)$ and $\sigma(\downarrow\uparrow)$, where the first arrow is for the beam and the second for the target, which shall be polarized in the $\uparrow$ direction. Then, $dN_\uparrow/dt=-N_\uparrow f_R dP_T\sigma(\uparrow\uparrow)$ and $dN_\downarrow/dt=-N_\downarrow f_R dP_T\sigma(\downarrow\uparrow)$. From Eqs. (2) and (3) one then obtains

$$\hat{\sigma}_R=-\tfrac{1}{2}[\sigma(\uparrow\uparrow)-\sigma(\downarrow\uparrow)]\equiv\tfrac{1}{2}\Delta\sigma , \tag{5}$$

or, in the case of longitudinal polarization,

$$\hat{\sigma}_{R,\|}=\tfrac{1}{2}\Delta\sigma_L=-2\pi\int_{\Theta_{\rm acc}}^{\pi/2}\frac{d\sigma}{d\Omega}A_{ll}\sin(\theta)d\theta , \tag{6}$$

and, for the transverse case,

$$\hat{\sigma}_{R,\perp}=\tfrac{1}{2}\Delta\sigma_T=-2\pi\int_{\Theta_{\rm acc}}^{\pi/2}\frac{d\sigma}{d\Omega}\tfrac{1}{2}(A_{nn}+A_{mm})\sin(\theta)d\theta . \tag{7}$$

Here, the A_{ii} are the spin correlation coefficients A_{00ii}, related to the difference of the scattering rates in the triplet and singlet state, and defined in Ref. [6] and the integration extends to $\pi/2$ only, as is required by the identity of the collision partners. It is important to note that the above spin-dependent, angle-integrated cross sections are *not* entirely due to the strong interaction. Rather, as we shall see in Sec. III, Coulomb-nuclear interference contributes significantly to the value of $\Delta\sigma_L$ and $\Delta\sigma_T$.

C. Contribution of small-angle scattering: $\hat{\sigma}_S$

Beam protons that scatter from the target by angles less than $\Theta_{\rm acc}$ remain in the ring, carrying out betatron oscillations around the equilibrium orbit. Eventually, the amplitude of these oscillations is damped by electron cooling. During the scattering event, the target polarization may be transferred to the projectile. The resulting change $\langle\Delta P\rangle$ of the polarization of the scattered particle approaches zero for small angles, $\theta\to 0$. The cross section, however, grows more rapidly; in fact, one finds that the product $\langle\Delta P\rangle(d\sigma/d\Omega)$ diverges with $1/\theta^2$ as $\theta\to 0$. As a consequence, small-angle scattering does affect the polarization of a stored beam, even though the limiting scattering angle $\Theta_{\rm acc}$ is very small (typically 1–10 mrad).

Let us for the moment discuss vertical target polarization. The angle between the scattering plane and the vertical direction shall be ϕ. The expectation value $\langle P'\rangle$ of the polarization of the scattered particle can then be written in terms of polarization observables, the polarization P_B and P_T of beam and target, and the angle ϕ. When averaging over ϕ, we assume that the experiment is cylindrically symmetric or that the acceptance angle $\Theta_{\rm acc}$ does not depend on ϕ. Then, terms linear in $\sin\phi$ or $\cos\phi$ vanish, averaging over ϕ gives $\langle\sin^2\phi\rangle=\langle\cos^2\phi\rangle=\frac{1}{2}$, and

$$\langle P'\rangle=\frac{P_B\frac{1}{2}(D_{nn}+D_{mm})+P_T\frac{1}{2}(K_{nn}+K_{mm})}{1+P_BP_T\frac{1}{2}(A_{nn}+A_{mm})} , \tag{8}$$

where, according to the definition given in Ref. [6], the K_{ii} are the spin-transfer coefficients K_{i00i} from target to projectile, the D_{ii} are the depolarization parameters D_{i0i0}, and the A_{ii} are the spin correlation coefficients A_{00ii}. The expectation value $\langle \Delta P \rangle$ of the change in polarization of a beam proton per scattering event is simply the difference $\langle P' \rangle - P_B$. For small angles, the denominator in Eq. (8) can be set to 1 and

$$\langle \Delta P \rangle = P_B \tfrac{1}{2}(D_{nn}+D_{mm}-2)+P_T\tfrac{1}{2}(K_{nn}+K_{mm}) - P_B^2 P_T \tfrac{1}{2}(A_{nn}+A_{mm}) . \quad (9)$$

As will be shown in Sec. III, one finds that for small angles $K_{ii} \approx A_{ii}$ and that $(D_{ii}-1)(d\sigma/d\Omega)$ is constant (and does not contribute to the singularity). Then, $\langle \Delta P \rangle$ reduces to

$$\langle \Delta P \rangle = \tfrac{1}{2}(A_{nn}+A_{mm})P_T(1-P_B^2) . \quad (10)$$

Compared with Eq. (3), we find for the corresponding transverse polarizing cross section,

$$\hat{\sigma}_{S,\perp} = 2\pi \int_{\theta_{\min}}^{\Theta_{\rm acc}} \frac{d\sigma}{d\Omega} \tfrac{1}{2}(A_{nn}+A_{mm})\sin(\theta) d\theta . \quad (11)$$

Here, $\theta_{\min}$ is the lower bound of the scattering angle, due to screening of the Coulomb potential at large impact parameter (see Sec. IV).

The result for longitudinal polarization is obtained by replacing $\frac{1}{2}(A_{nn}+A_{mm})$ by A_{ll}:

$$\hat{\sigma}_{S,\parallel} = 2\pi \int_{\theta_{\min}}^{\Theta_{\rm acc}} \frac{d\sigma}{d\Omega} A_{ll} \sin(\theta) d\theta . \quad (12)$$

D. Contribution of polarized electrons: $\hat{\sigma}_E$

A polarized, internal atomic hydrogen target in a pure spin state, by necessity, contains polarized electrons. The spins of protons and electrons are aligned either in the same direction or opposite to each other, depending on the substate selected by the polarized-atom source that is used to generate the target. For opposite spins (atomic spin zero), a strong magnetic field is required to decouple the spins of the proton and electron from each other [7] in order to maintain their alignment.

A recent calculation [8] showed that a polarized electron target can significantly affect the polarization of a stored proton beam. In this calculation it was found that the cross section for spin transfer from target to projectile is relatively large because of the interference between the hyperfine and the Coulomb amplitude. Atomic screening of the Coulomb field restricts the scattering to momentum transfers larger than 1 over the screening distance (here taken as the Bohr radius, $a_0 = 5.3 \times 10^4$ fm). Then the energy transfer is larger than the binding energy of the hydrogen atom; thus atomic effects can be ignored and the electrons are treated as free particles.

The maximum laboratory angle by which a proton can be scattered by an electron at rest is $m_e/m_p = 0.54$ mrad with m_p, m_e the masses of the proton and the electron, respectively. Since this is well within the acceptance angle of any storage ring, the scattered protons remain in the ring. Therefore, we are interested in the *total* cross section, integrated over the full range of scattering angles. The spin-transfer cross section and thus the cross section for polarizing a beam of protons by interaction with longitudinally polarized, stationary electrons is obtained from Ref. [8] as

$$\hat{\sigma}_{E,\parallel} = -\left[\frac{4\pi\alpha^2(1+\lambda_p)m_e}{p^2 m_p}\right] C_0^2 \left[\frac{\nu}{2\alpha}\right] \times \sin\left[\frac{2\alpha}{\nu}\ln(2pa_0)\right] . \quad (13)$$

Here, p is the center-of-mass momentum, α is the fine structure constant, $\lambda_p = 1.793$ is the anomalous moment of the proton, and ν is the lab velocity of the projectile. The minus sign in Eq. (13) indicates that the induced proton polarization is *opposite* to the direction of the electron spin. Equation (13) takes into account the distortion of the wave functions by the Coulomb interaction. It has two contributions. One arises from the value $C_0^2 = 2\pi\eta/[\exp(2\pi\eta)-1]$ with $\eta = -\alpha/\nu$ of the s-wave Coulomb wave function at $r=0$, where the (short-ranged) hyperfine amplitude is evaluated, and the other from the angle-dependent phase of the Coulomb amplitude. At 23 MeV the effect of distortion enhances the spin-transfer cross section by 11% over the plane-wave result. For polarization transfer in the transverse direction, one finds [8]

$$\hat{\sigma}_{E,\perp} = \tfrac{1}{2}\hat{\sigma}_{E,\parallel} . \quad (14)$$

III. POLARIZATION OBSERVABLES IN $p+p$ SMALL-ANGLE SCATTERING

In order to evaluate the polarizing cross sections $\hat{\sigma}_R$ and $\hat{\sigma}_S$ one needs to know the relevant polarization observables for $p+p$ elastic scattering at angles that are of the order of the acceptance angle $\Theta_{\rm acc}^*$ (typically 1 to 10 mrad).

The elastic scattering of protons from protons is completely described by five complex amplitudes which depend on angle and energy. Here, we use helicity amplitudes M_i ($i=1,\ldots,5$) as they are defined in Eq. (2.23) of Ref. [6]. Each amplitude can be decomposed into a hadronic part h_i and a contribution Φ_i from the electromagnetic interaction or $M_i = h_i + \Phi_i$. The scattering cross section $d\sigma/d\Omega$ (for short, σ) in terms of these helicity amplitudes is given by [6]

$$\sigma \equiv \frac{d\sigma}{d\Omega} = \tfrac{1}{2}(|M_1|^2+|M_2|^2+|M_3|^2+|M_4|^2+4|M_5|^2) . \quad (15)$$

Any other (polarization) observable X, when multiplied by the cross section σX is a bilinear sum over terms $M_i^* M_j$. A complete list of observables in terms of helicity amplitudes is given in Table VI of Ref. [6].

Consider an observable σX, which, for small θ, is proportional to $1/\theta$. An integral over the solid angle Ω of the ring acceptance is then of the order of Ω and thus

negligible. On the other hand, observables σX that are proportional to $1/\theta^2$ lead to an integrand that diverges at $\theta=0$, resulting in a significant contribution for small θ.

In the limit $\theta\to 0$, h_1, h_2, and h_3 are constant, while h_4 and h_5 are proportional to θ^2 and θ, respectively. The Coulomb amplitudes $\Phi_2=-\Phi_4$ are constant, Φ_5 scales with $1/\theta$, and $\Phi_1=\Phi_3$ are proportional to $1/\theta^2$. It is easy to see that only terms containing a product of Φ_1 (or Φ_3) with any combination of h_1, h_2, and h_3 diverge with $1/\theta^2$ (ignoring a possible small contribution from $|\Phi_5|^2$). Retaining only such terms in the expressions of Table VI of Ref. [6], yields

$$\tfrac{1}{2}\sigma(A_{nn}+A_{mm})=\tfrac{1}{2}\sigma(K_{nn}+K_{mm})=\mathrm{Re}(h_2\Phi_1^*)\ , \tag{16}$$

and

$$\sigma A_{ll}=\sigma K_{ll}=\mathrm{Re}[(h_3-h_1)\Phi_1]\ , \tag{17}$$

where h_i stands for the corresponding, purely hadronic helicity amplitude at $\theta=0$. Numerical values for these amplitudes can be obtained (in units of femtometers), for instance, from the interactive $p+p$ data base SAID [9], which has the provision to calculate amplitudes without any Coulomb effects. Their normalization is compatible with Eq. (15), when the output from SAID is multiplied by 2. Also, the ordering of the five SAID amplitudes differs from Ref. [6] (the SAID labels a,b,c,d,e correspond to our subscripts 1,5,3,2,4, respectively). Numerical values for the forward amplitudes h_2 and (h_3-h_1) were obtained from SAID, using the global solution SM89. Different phase shift solutions gave similar results; for instance, h_2 at 23 MeV with solutions SM89 and CO25 differ by only a few percent. The forward amplitudes which will be used in the following are shown in Fig. 1 as a function of energy.

Expressions for the five Coulomb amplitudes Φ_i, valid at low momentum transfer, are given for instance in the appendix of Ref. [10]. Here, we are only concerned with the amplitude Φ_1. We ignore the contribution from the electromagnetic form factor of the proton, which is unimportant at small θ, and choose the normalization such

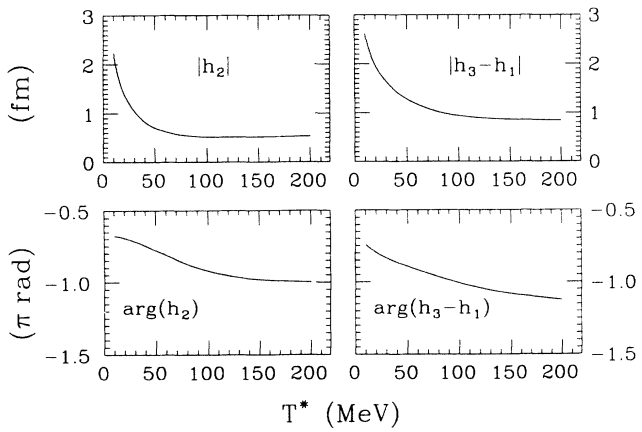

FIG. 1. Modulus and phase of the forward amplitudes $h_2(0)$ [and $h_3(0)-h_1(0)$] for $p+p$ scattering, as a function of laboratory energy T^*. The values are obtained from SAID [10], using the global solution SM89.

that Eq. (15) is the Rutherford cross section when the hadronic amplitudes are set to zero. This results in

$$\Phi_1(s,\theta)=-\alpha\frac{s-2m_p^2}{\sqrt{s}}\frac{e^{i\delta(s,\theta)}}{p^2\theta^2}\ , \tag{18}$$

with $s=2m(2m+T^*)$, where T^* is the proton laboratory energy and $p=\frac{1}{4}(s-4m_p^2)^{1/2}$ is the center-of-mass momentum. The phase angle $\delta(s,\theta)$, is given by Eq. (2.9) of Ref. [10] as

$$\delta(s,\theta)=-\alpha\frac{s-2m_p^2}{\sqrt{s(s-4m_p^2)}}[0.5772+\ln(b_c p^2\theta^2)]\ , \tag{19}$$

where b_c is determined by a fit to elastic scattering data. For the present purpose, it is sufficient to set b_c to a constant value, $b_c=9.94\times10^{-6}\ \mathrm{MeV}^{-2}$.

Polarization observables calculated for small angles (a few degrees) from the hadronic forward amplitude and the analytic expression for the Coulomb amplitude given above agree within a few percent with the same observables as listed in the SAID data base.

IV. RESULTS AND COMPARISON WITH EXPERIMENT

A. Polarization of a 23-MeV proton beam

In Sec. II we have identified three distinct mechanisms that contribute significantly to the polarization of a stored proton beam when it interacts with a polarized hydrogen target.

The first is caused by selective removal (scattering beyond Θ_{acc}) from one of the spin substates of the beam. The corresponding polarizing cross section $\hat{\sigma}_{R\perp}$ [Eq. (7)] (with the appropriate transformation to the laboratory system) was evaluated as follows. From Θ^*_{acc} to $\theta^*=3°$, the integrand was calculated using the small-angle expression, Eq. (16). For the remainder of the angular range, the integrand has been obtained pointwise from the data base SAID [9]. The integration was carried out numerically. The result, as a function of Θ^*_{acc}, is shown as a dashed line in Fig. 2. For $\Theta^*_{\mathrm{acc}}=4.4$ mrad (the acceptance angle of the TSR; see Sec. I B), one finds $\hat{\sigma}_{R\perp}=83$ mb. When the calculation is repeated without the Coulomb interaction, the result agrees with the purely hadronic, spin-dependent cross section of $\frac{1}{2}\Delta\sigma_T=122$ mb (which can also be calculated from the imaginary part of the forward amplitude h_2 by virtue of the optical theorem). It is obvious that Coulomb-nuclear interference causes an important contribution to the spin-dependent removal cross section.

The second contribution $\hat{\sigma}_{S\perp}$, from small-angle scattering of protons, which subsequently remain stored in the ring, follows easily from Eqs. (11) and (16), setting $\theta^*_{\mathrm{min}}\approx 1/(p^*a_0)$, where a_0 is the Bohr radius and p^* is the lab momentum. For $\Theta^*_{\mathrm{acc}}=4.4$ mrad, one finds $\hat{\sigma}_{S\perp}=52$ mb. The combined, hadronic effect $\hat{\sigma}_{R\perp}+\hat{\sigma}_{S\perp}$ as a function of Θ^*_{acc} is shown as a dash-dot line in Fig. 2.

The third contribution $\hat{\sigma}_{E\perp}$ is due to the polarized electrons in the target. From Eqs. (13) and (14) one finds

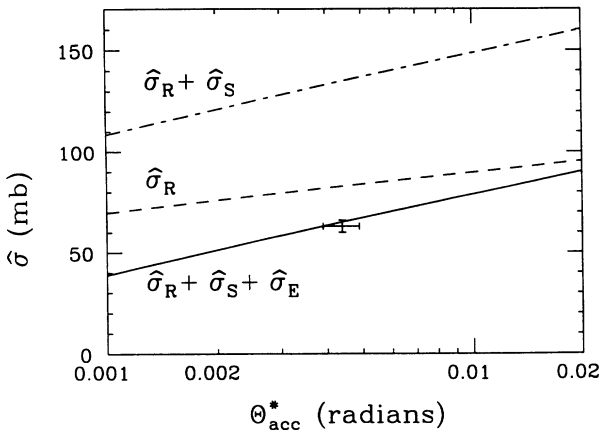

FIG. 2. Polarizing cross section for a polarized hydrogen target and a 23-MeV proton beam as a function of the laboratory acceptance angle Θ^*_{acc}. The dashed line is the removal cross section $\hat{\sigma}_{R\perp}$, which, without Coulomb interaction, would be 122 mb, independent of Θ^*_{acc}. The entire hadronic contribution is shown by the dash-dotted line. The solid line is obtained if the effect of the target electrons (polarized in the same direction as the protons) is included. The result of the TSR experiment [4] at the measured TSR acceptance angle [5] is also shown.

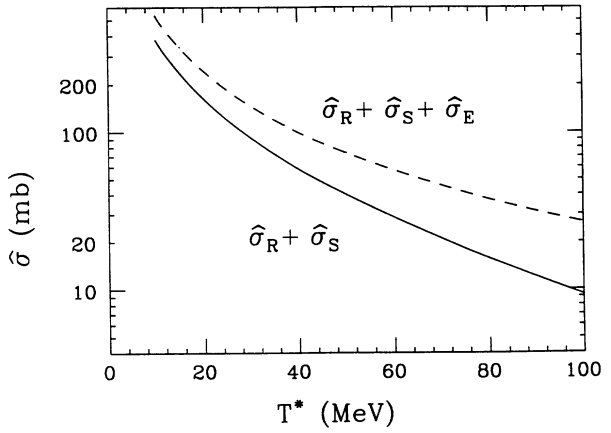

FIG. 3. Transverse polarizing cross section for a polarized hydrogen target and a proton beam as a function of the laboratory energy T^*. The calculation is for a ring acceptance angle of $\Theta^*_{acc}=4.4$ mrad. The solid line shows the contribution from the polarized target protons alone. The dashed line includes the effect of atomic electrons when they are polarized opposite to the protons.

$\hat{\sigma}_{E\perp}=-70$ mb, independent of Θ^*_{acc}, for electrons that are polarized in the same direction as the protons, as was the case in the TSR experiment. In this case, the effect from the electrons is opposite to that of the polarized protons. The polarizing cross section from all three sources $\hat{\sigma}_{R\perp}+\hat{\sigma}_{S\perp}+\hat{\sigma}_{E\perp}$ as a function of Θ^*_{acc} is shown as a solid line in Fig. 2.

Also indicated in Fig. 2 is the experimental result [4] and the measured acceptance angle with its uncertainty [5]. As can be seen from Fig. 2, the expected polarizing cross section is in excellent agreement with the experiment, especially if one takes into account that the effective acceptance angle for a finite-emittance beam is expected to be somewhat smaller than the geometric value.

B. Energy dependence of the polarizing cross section

As the bombarding energy increases, the hadronic amplitudes are decreasing, as can be seen from Fig. 1. In addition, the Coulomb amplitude also decreases. Thus, the polarizing effect of a polarized internal hydrogen target quickly becomes small. In Fig. 3 the hadronic polarizing cross section for a transversely polarized target $\hat{\sigma}_{R\perp}+\hat{\sigma}_{S\perp}$ as a function of bombarding energy is shown as a solid line; the acceptance angle was taken to be $\Theta^*_{acc}=4.4$ mrad. The cross section that results when the contribution from the electrons is included is shown here as a dashed line for the case where the electrons are polarized *opposite* the protons. This would require that target atoms be prepared in hyperfine state 2 (see Ref. [7]). In practice, this can be achieved by separating atoms in states 1+2 by spin separation in a multipole field, followed by an rf transition between states 1 and 3, after which another multipole magnet removes state 3. A "strong" magnetic field (of the order of 0.1 T) has to be present at the target location in order to decouple the spins of the electron and the proton. Figure 4 shows the same for a target that is polarized *along* the beam direction. Note that in this case the spin closed orbit, i.e., the direction in which the beam polarization is stable, must also be in the longitudinal direction, which requires additional magnetic elements in the ring lattice (so-called snakes).

While the beam is being polarized, its intensity decreases exponentially. At medium energies the most important mechanism for beam loss is Rutherford scattering. Thus, it may be argued that in order to select an optimum beam energy, one should consider the ratio of the polarizing cross section to the Rutherford cross section. This ratio exhibits a maximum near 50 MeV if only the hadronic mechanisms are taken into account. However,

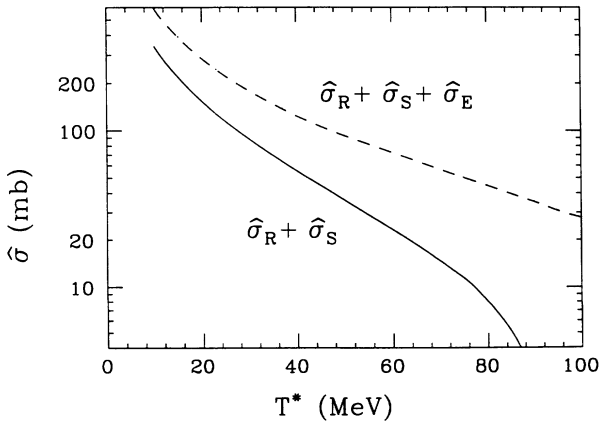

FIG. 4. Longitudinal polarizing cross section. Otherwise, the caption of Fig. 3 applies.

the electronic spin-transfer cross section decreases less rapidly than the Rutherford cross section. Thus, the higher the energy, the higher the beam intensity that survives after a given value of the beam polarization has been reached. The optimum energy in this case is given by practical considerations involving duration of the polarizing phase.

V. CONCLUSIONS

In this paper we have studied the change in polarization of an ensemble of stored particles, which is induced by the presence of a polarized, internal target. We find that the polarization change is achieved not only by selective removal of particles but, to a large extent also by manipulating an existing ensemble *while maintaining it.*

We find that the one existing measurement [4] is in agreement with our calculation. We have also calculated the energy dependence of the polarizing cross section for polarized atomic targets in different spin states. We find that at the same energy and for the same acceptance angle as for the TSR experiment the polarizing effect would have been larger if the polarized target were used differently. For instance, for a longitudinally polarized target in a strong magnetic field and in a spin state where the electrons and the protons are oppositely polarized, the polarizing effect is 3.8 times larger than in the case of the TSR experiment. The intensity of the beam after polarization can be increased by raising the beam energy because with increasing energy the Rutherford cross section falls more rapidly than the polarizing cross section. The optimum choice for the beam energy is given by the beam lifetime without target.

ACKNOWLEDGMENTS

We are indebted to W. Haeberli for many helpful suggestions and to S. Howell for assistance with numerical calculations. This work has been supported in part by the National Science Foundation under Grant No. NSF PHY 93-14783.

[1] R. E. Pollock, Annu. Rev. Nucl. Sci. **41**, 357 (1991).
[2] M. A. Ross, W. K. Pitts, W. Haeberli, H. O. Meyer, S. F. Pate, R. E. Pollock, B. v. Przewoski, T. Rinckel, J. Sowinski, F. Sperisen, and P. V. Pancella, Nucl. Instrum. Methods Phys. Res. Sect. A **326**, 424 (1993).
[3] T. O. Niinikoski and R. Rossmanith, Nucl. Instrum. Methods Phys. Res. Sect. A **255**, 460 (1987).
[4] F. Rathmann, C. Montag, D. Fick, J. Tonhaeuser, W. Brueckner, H.-G. Gaul, M. Grieser, B. Povh, M. Rall, E. Steffens, F. Stock, K. Zapfe, B. Braun, G. Graw, and W. Haeberli, Phys. Rev. Lett. **71**, 1379 (1993).
[5] C. Montag, Diplomarbeit, Philipps-Universität Marburg, 1993.
[6] J. Bystricky, F. Lehar, and P. Winternitz, J. Phys. (Paris) **39**, 1 (1978).
[7] W. Haeberli, Annu. Rev. Nucl. Sci. **17**, 373 (1967).
[8] C. J. Horowitz and H. O. Meyer, Phys. Rev. Lett. (to be published).
[9] R. A. Arndt, L. D. Roper, R. A. Bryan, R. B. Clark, B. J. VerWest, and P. Signell, Phys. Rev. D **28**, 97 (1983), and the data base SAID mentioned therein.
[10] R. Jakob and P. Kroll, Z. Phys. A **344**, 87 (1992).